NATIONAL AERONAUTICS AND SPACE ADMINISTRATION

Technical Report No. 32-910

Application of Ground Test Acoustic Simulations of Liftoff and Transonic Vibration to Actual Ranger Flight Vibration Data

Marc C. Trummel

W. Shipley, Manager
Environmental Requirements Section

JET PROPULSION LABORATORY
CALIFORNIA INSTITUTE OF TECHNOLOGY
PASADENA, CALIFORNIA

May 1, 1966

Prepared Under Contract No. NAS 7-100
National Aeronautics & Space Administration

CONTENTS

TABLE

CONTENTS (Cont'd)

FIGURES

CONTENTS (Cont'd)

FIGURES (Cont'd)

ABSTRACT

During the *Ranger* flight program, only a limited amount of in-flight vibration data was obtained. In order to expand the usefulness of this data, a ground test was conducted in which a large number of vibration and acoustic measurements were made. The test approximated, by the use of acoustic fields, the vibration excitation mechanisms existing at the flight periods of maximum vibration: liftoff and transonic. By using the ground test data in conjunction with the flight data, the following results were achieved: (1) The nature of the vibration caused by the two excitation modes was determined, and the effect of flight accelerometer characteristics on measured vibration was analyzed. (2) A method of predicting flight vibration levels was developed and, by comparison with the actual flight data, was shown to be adequate at higher frequencies, but overly conservative at lower frequencies. (3) The flight vibration environment at the *Ranger* spacecraft feet and at two general classes of equipment locations on the spacecraft was estimated and shown to be adequately covered by vibration test specifications.

I. INTRODUCTION

The limited availability of high-frequency telemetry channels restricted the number of in-flight, high-frequency vibration and acoustic measurements made during the *Ranger* Project. To make the most meaningful use of the limited available data, ground tests on a dynamic model of the *Ranger* Block III spacecraft (*Rangers VI* through *IX*) were conducted using a large amount of acoustic and vibration instrumentation. These tests were intended to simulate the vibration excitation mechanisms at liftoff and transonic flight, as experienced by an actual *Ranger* flight, by the use of properly controlled acoustic fields. The results of these ground tests were combined with the actual flight data with the following objectives:

(1) To discover the effects of the different types of vibration excitation modes at liftoff and transonic and the various types of flight accelerometer mounting configurations.

(2) To develop a method of predicting spacecraft vibration environment using an estimate of the acoustic environment and to compare a prediction of *Ranger* environment using this technique to flight data.

(3) To estimate the flight vibration environment at the spacecraft feet and to compare this estimate with the specified vibration test.

(4) To estimate the flight vibration environment at the spacecraft assemblies and to compare this estimate with the specified vibration test.

II. *RANGER* FLIGHT DATA

A. Grouping by Configurations

High-frequency flight vibration data is available from eight of the nine *Ranger* flights. On all of the eight instrumented flights, an accelerometer was located in the spacecraft adapter region; on the last two flights (*Rangers VIII* and *IX*), an additional accelerometer was located on the spacecraft bus. The high-frequency accelerometers in the adapter section were attached by brackets bolted to one of the six "pork chop" supports. The spacecraft bus accelerometer on *Rangers VIII* and *IX* was mounted on a specially designed bolt plate used by one of the attaching bolts at the lower-left corner of the Case IV assembly.

Reference 1 presents a detailed description of the flight vibration measurement program and includes discussions

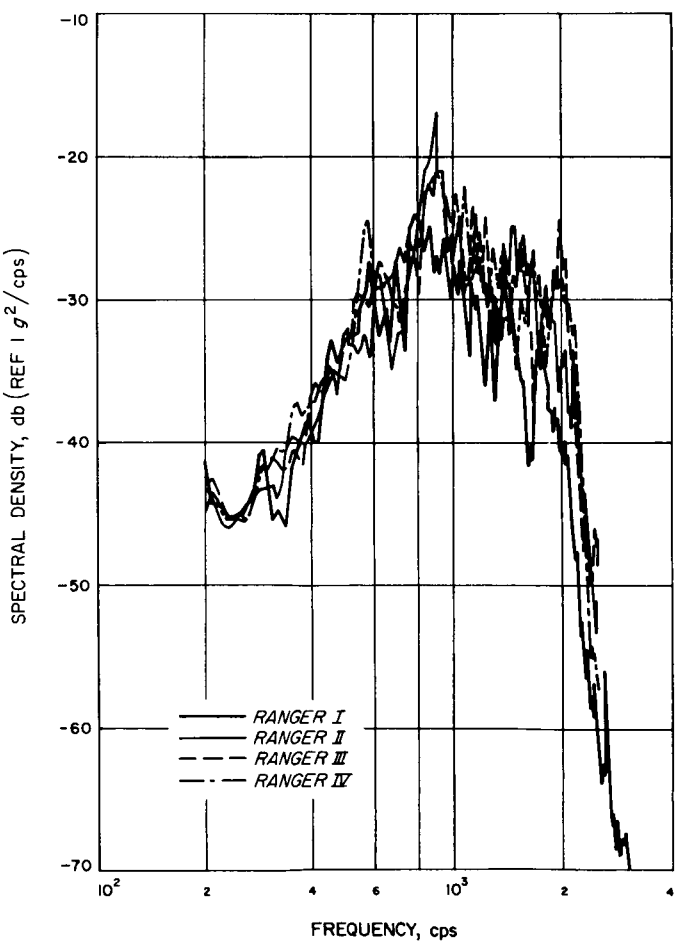

Fig. 1. *Ranger I–IV* flight PSD's at liftoff: adapter accelerometer

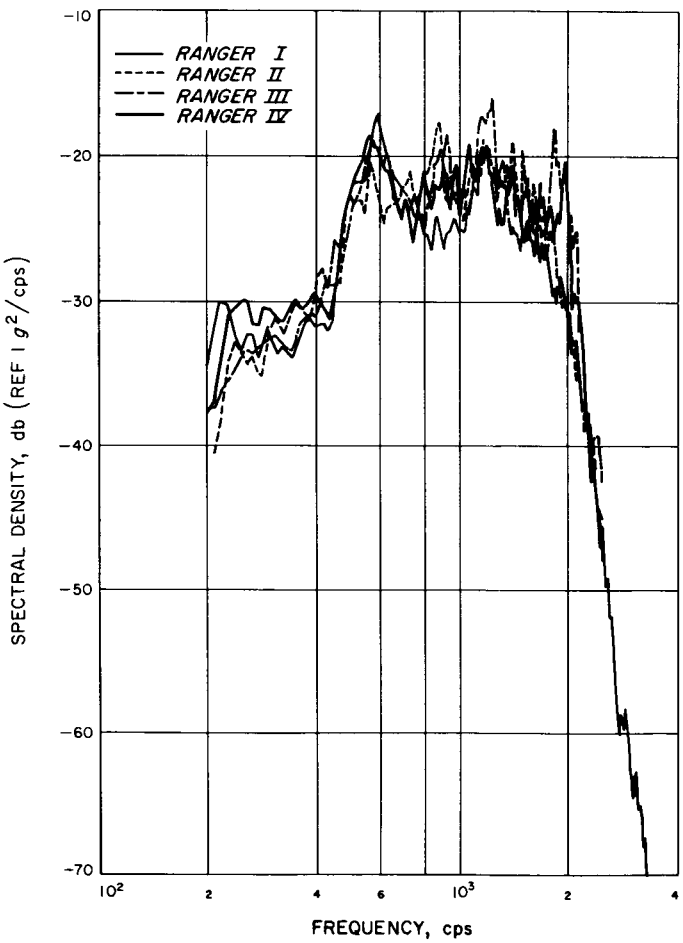

Fig. 2. *Ranger I–IV* flight PSD's at transonic: adapter accelerometer

of telemetry as well as complete descriptions of accelerometer physical locations. Unfortunately, the eight adapter measurements represent four different configurations (or types) of accelerometer mounting methods, each of which must be considered separately in an analysis (*Rangers I–IV*, *Rangers VI* and *VIII*, *Ranger VII*, and *Ranger IX*). These sets of measurements with their significant differing characteristics are listed in Table 1.

B. Adapter Region

The actual flight data is presented as power spectral densities (PSD) from a 2-sec time sample at the maximum wide-band vibration point found at liftoff and transonic. The analysis has a 20-cps resolution resulting in 80 degrees of freedom. The data is shown in Figs. 1 through 6. The flight-to-flight consistency may be seen by examining the radial data from the *Ranger I–IV* flights (Figs. 1 and 2). Of particular significance is repeatability of the data below 500 cps. Above this frequency, there is some variation of the magnitude and frequencies of the "peaks and valleys" in the data; e.g., the liftoff data for *Ranger III* (Fig. 1) shows a peak at 900 cps (approximately 6 db above the other three flights). Similar differences may be found at other points on the liftoff data and on the transonic data (Fig. 2).

Table 1. Groupings of *Ranger* flight vibration measurements

Set	Sensitive axis	Type of bracket	Comment
Rangers I–IV	Radial	Blocks I and II	Sterilization diaphragm used
Rangers VI, VIII	Radial	Block III	Bracket is closer to adapter skin: no sterilization diaphragm
Ranger VII	Axial	Block III	Same bracket as *Rangers VI, VIII*: no sterilization diaphragm
Ranger IX	Axial	Block III (stiffened)	Tab holding accelerometer is thicker and supporting web is added: no sterilization diaphragm

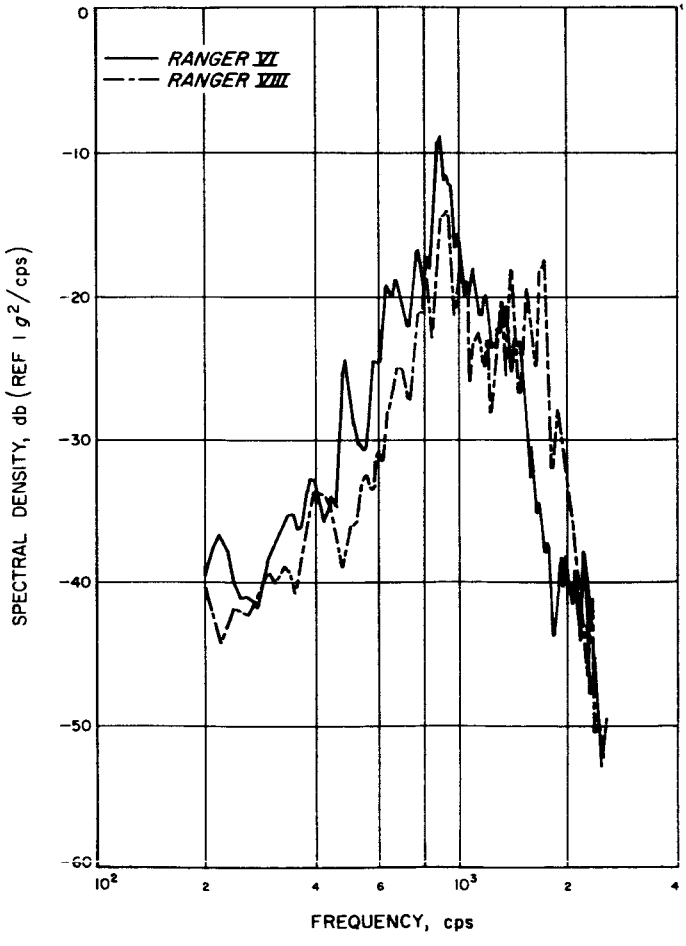

Fig. 3. *Ranger VI* and *VIII* flight PSD's at liftoff: adapter accelerometer

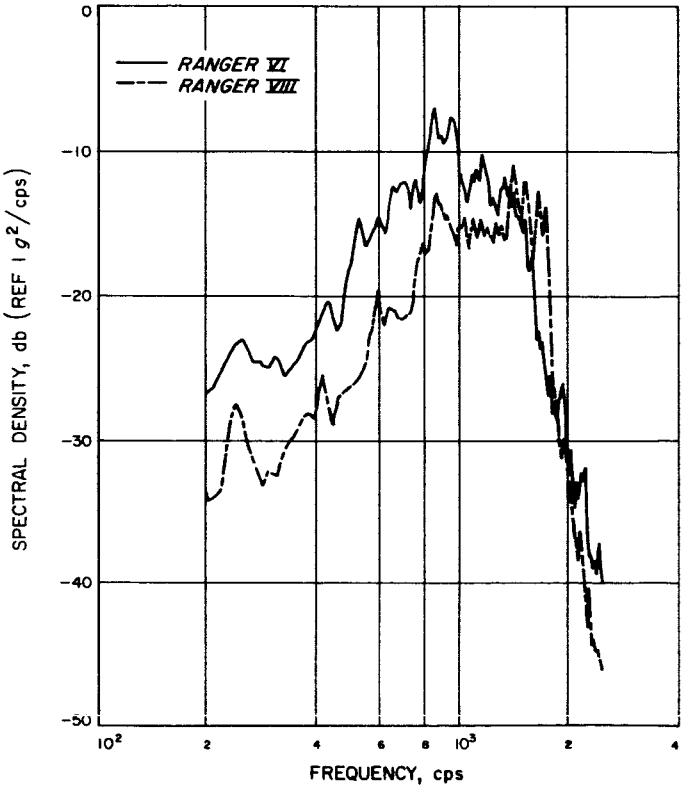

Fig. 4. *Ranger VI* and *VIII* flight PSD's at transonic: adapter accelerometer

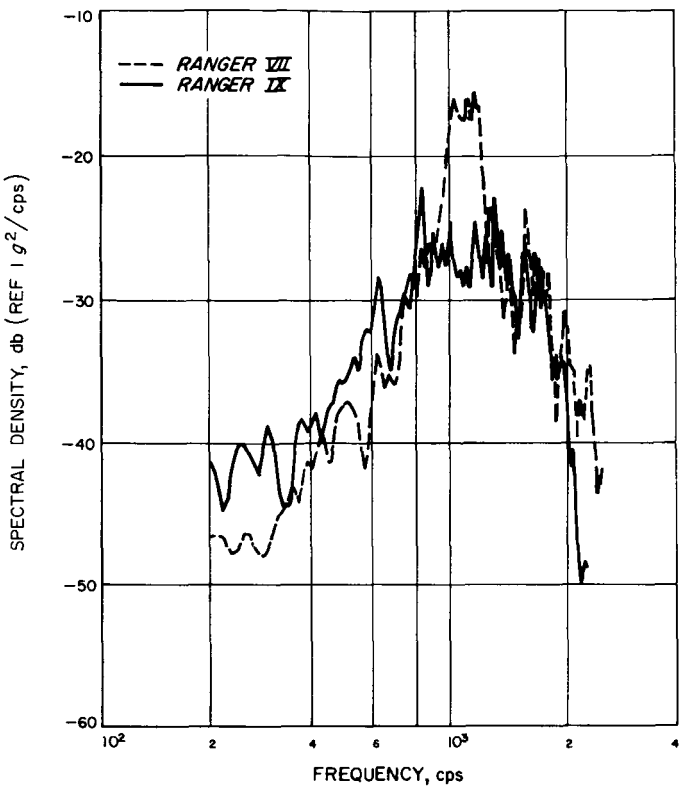

Fig. 5. *Ranger VII* and IX flight PSD's at liftoff: adapter accelerometer

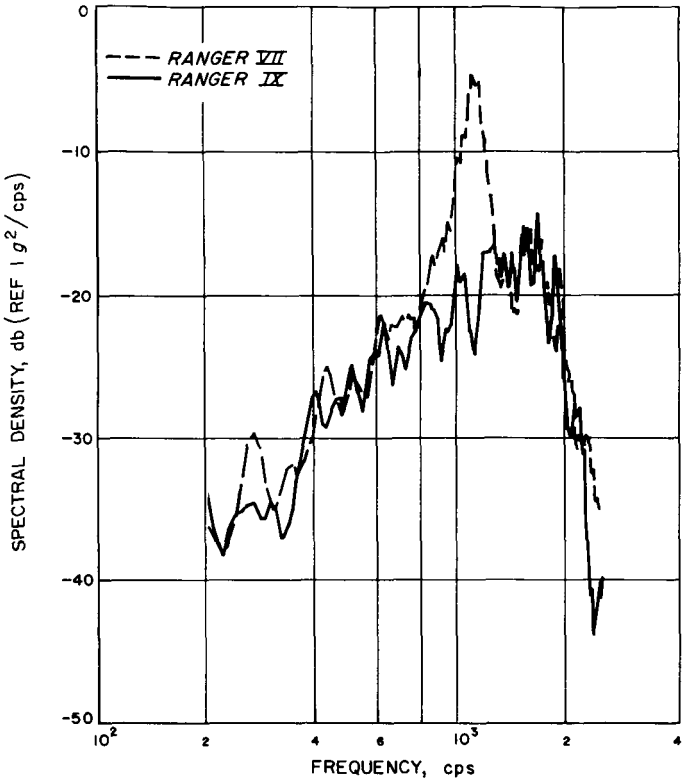

Fig. 6. *Ranger VII* and IX flight PSD's at transonic: adapter accelerometer

The radial data from *Rangers VI* and *VIII*, taken on identical accelerometer mounting blocks (Figs. 3 and 4), indicate larger variations than would be predicted based on the consistency of the data from *Rangers I* through *IV*. While some variation between the data from *Ranger VI* and *Ranger VIII* is to be expected, the gross differences are excessive in the region below 500 cps, and some doubt must be cast on the validity (or at least on a simple interpretation) of both *Ranger VI* and *VIII* flight data. The data below 500 cps from *Rangers I* through *IV* is found to be in much closer agreement with the *Ranger VIII* data than with that of *Ranger VI*.

The data from *Rangers VII* and *IX* must be considered as representing separate groups because of the significant stiffening of the accelerometer mount on *Ranger IX* (Figs. 5 and 6). The reason for the stiffening was the 1000- to 1200-cps resonance apparent in the *Ranger VII* data; the *Ranger IX* data and laboratory tests of a *Ranger IX* mounting block indicate that the resonance has been raised above 2000 cps. Again, in the 250- to 500-cps range, both flights (even though they are axial measurements) compare well with each other and with the *Ranger I–IV* and *Ranger VIII* data.

C. Spacecraft Bus Region

A second high-frequency accelerometer was flown on *Rangers VIII* and *IX*. Vibration PSD's from these accelerometers taken at the same times as the adapter accelerometers are shown in Figs. 7 and 8. Agreement between the two flights is good up to 800 cps; at higher frequencies, the *Ranger IX* data shows a higher response at transonic. This is not fully explained, as the accelerometer mounting systems are nominally identical.

D. Ground Measurement of Acoustic Field

Ground measurements of the acoustic field generated by the rocket motors at liftoff were made on the *Ranger VI–IX* flights. The measurement program is discussed in detail in Ref. 1. To actually define the liftoff acoustic environment from these particular measurements presents significant problems which result in a limited usefulness. The physical conditions of the measurements which cause analysis problems are:

(1) The booster and spacecraft move during the high noise period, while the microphone locations are fixed.

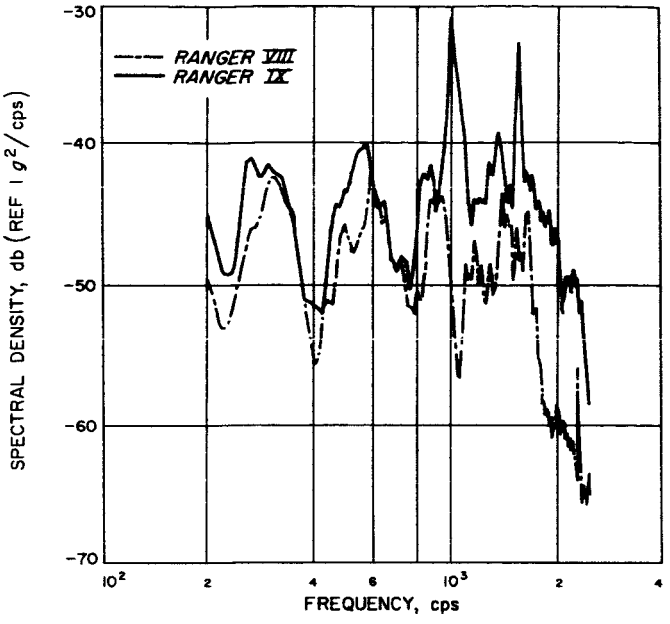

Fig. 7. *Ranger VIII* and *IX* flight PSD's at liftoff: spacecraft bus accelerometer

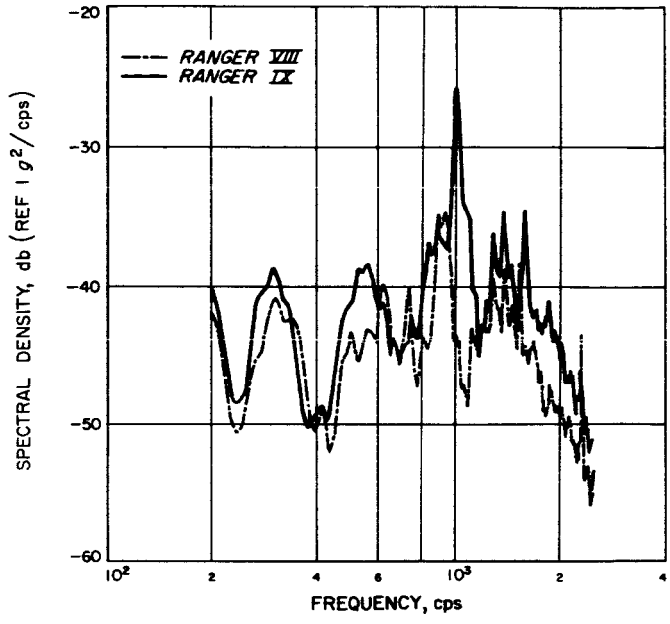

Fig. 8. *Ranger VIII* and *IX* flight PSD's at transonic: spacecraft bus accelerometer

(2) The location of the microphones is partially in the acoustic shadow of the launch vehicle, since they are located on the umbilical tower (partially behind and below the spacecraft).

In addition to these problems, other difficulties were encountered such as incorrect data and actual cutting of microphone leads; however, some meaningful data was extractable. Figure 9 shows pressure spectrum level (PSL) measurements from a tower microphone on the *Ranger VI–VIII* launches. Shown for comparison is an estimate of the actual spacecraft acoustic environment (Ref. 2). This estimate, (with ⅓-octave resolution) was made by use of actual static firing measurements, as well as purely analytic techniques. The *Ranger* data is in reasonable agreement with that of the estimate, although it is generally lower, possibly showing the effects of shadowing and increased distance from the sound source. It appears reasonable to use the estimate as the launch liftoff environment at the nearest point of the spacecraft to the sound source.

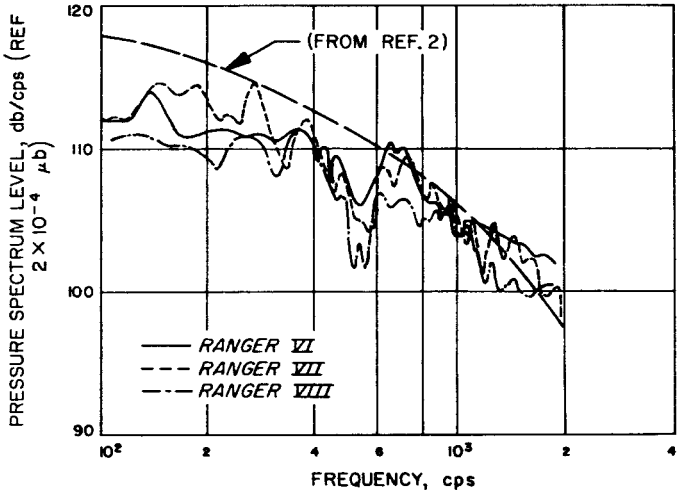

Fig. 9. *Ranger* liftoff external acoustic noise-field measurements

III. RESULTS FROM GROUND ACOUSTIC TEST

Because of the very limited high-frequency vibration data from the actual *Ranger* flights, it was necessary to conduct a ground test to further understand the distribution of vibration over the spacecraft and the relationship of vibration to the sound field. Although the vibration excitation mechanisms at liftoff and transonic flight may be classed as "acoustic" in nature, the characteristics of the exciting pressure fields are markedly dissimilar. The ground test was designed to simulate, by use of acoustic fields, both types of mechanisms in order to determine spacecraft vibration sensitivity to each one. The test and its physical setup are described in detail in Ref. 3. The *Ranger* vehicle used in the test was a structural test model (STM); structural simulation was complete to the subassembly level. Reference 3 shows the STM to be a good dynamic model because gains measured on the STM during the ground test compared well with gains measured on two spacecraft during actual launches.

A. Measurement of Acoustic Acceptances at Flight Accelerometer Locations

During these tests, the high-frequency flight accelerometer mounting configurations used on the *Ranger I–IV* flights, *Ranger IV* and *VIII* flights, and the *Ranger VII* flight were simulated. At that time, the *Ranger IX* accelerometer mount (a stiffened version of the *Ranger VII* mount) was not yet designed or simulated. To compare the various mounting configurations and the effects of

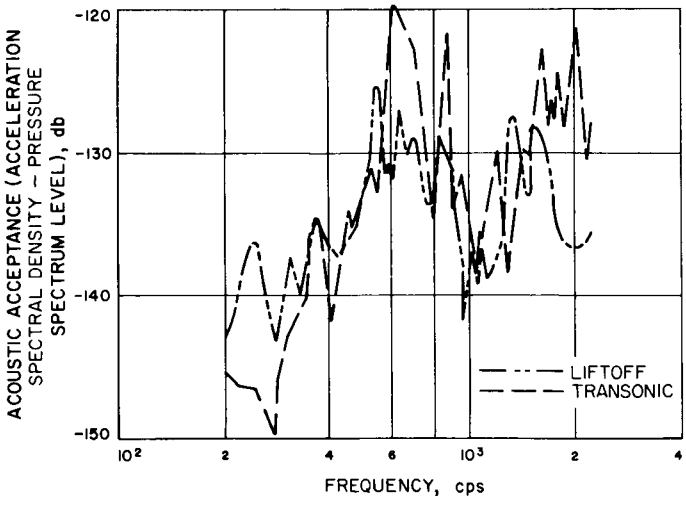

Fig. 10. Acoustic acceptance: *Ranger I–IV* flight accelerometer

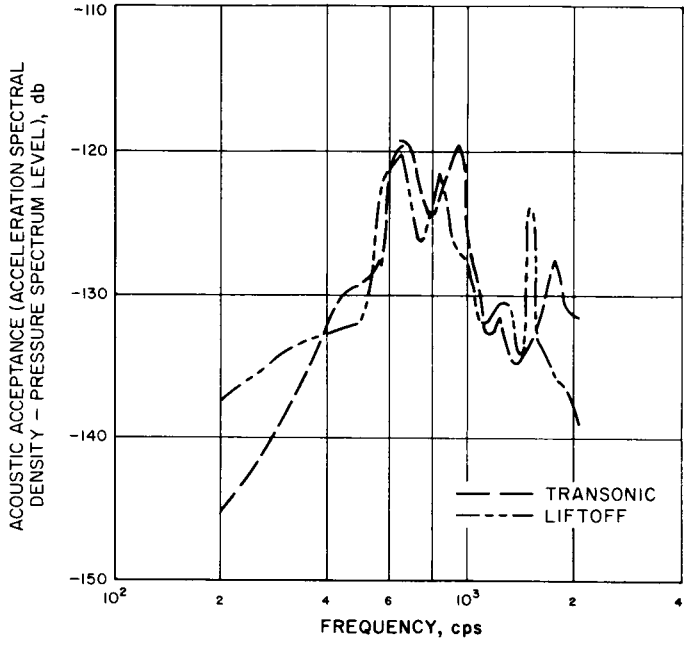

Fig. 11. Acoustic acceptance: *Ranger VI and VIII* flight accelerometer

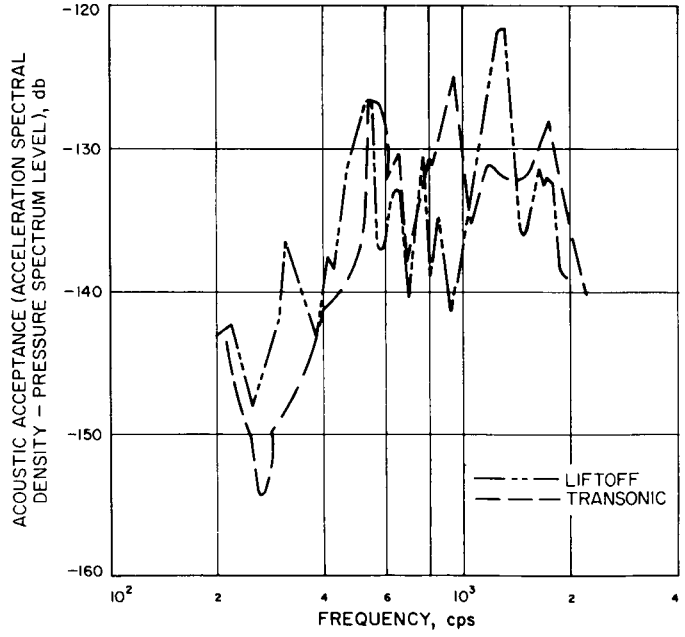

Fig. 12. Acoustic acceptance: *Ranger VII* flight accelerometer

the differing modes of vibration excitation (at liftoff and transonic), the acoustic acceptances (AA) at the various flight accelerometer locations were calculated for liftoff and transonic simulations. As described in Ref. 3, the reference measurement of the exciting noise field was the average of three microphones equally spaced external to the adapter (approximately 6 in. from the skin).

Figures 10, 11, and 12 compare the measured AA for the liftoff and transonic simulation of the three types of flight accelerometer mounts. There is good agreement between measured AA under both modes of excitation, particularly at intermediate frequencies between 300 and 600 cps. The axial measurement (*Ranger VII*) shows the most deviation; however, if the higher frequency resonance appearing at 920 cps for transonic and at 1300 cps for liftoff is considered to be the same (but shifted in frequency), then even the data in Fig. 12 shows good agreement.

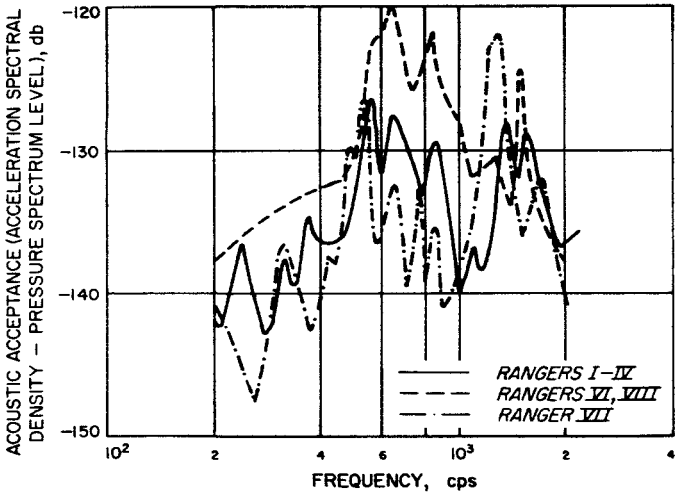

Fig. 13. Acoustic acceptance: flight accelerometer at liftoff

In order to illustrate the differences between the three mounting configurations, the curves from Figs. 10, 11, and 12 have been regrouped by mode of excitation (liftoff or transonic) on Figs. 13 and 14. As can be seen from the figures, the *Ranger VI* and *VIII* mount AA are generally somewhat higher than those of *Rangers I–IV* or the *Ranger VII* mount in the 600- to 1000-cps region (particularly in the liftoff simulation). The *Ranger VII* mount AA shows a resonance at 1300 cps in the liftoff simulation, but not in the transonic simulation. Generally, the *Ranger VII* mount is lower, indicating less vibration sensitivity than the *Ranger I–IV* mount.

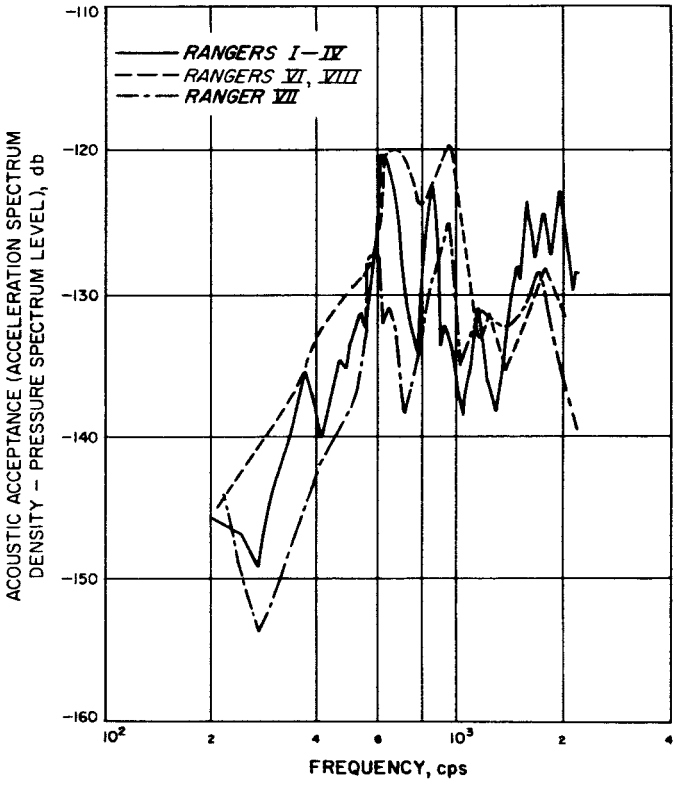

Fig. 14. Acoustic acceptance: flight accelerometer at transonic

IV. PREDICTION OF IN-FLIGHT VIBRATION LEVEL AT FLIGHT ACCELEROMETER LOCATIONS

Because of the remoteness of the spacecraft from the rocket engines, the source of vibration in the *Ranger* spacecraft region is primarily acoustic. The acoustic field at liftoff is generated by the rocket motor exhaust turbulence and at transonic by the areodynamic phenomena of flow separation and buffet. The AA data obtained from the ground tests relates the induced vibration to a measure of the acoustic field producing it. Provided that the acoustic field can be defined, AA data, therefore, permits a prediction of vibration expected in flight. In actuality,

reasonably accurate estimates of the *liftoff* acoustic field at the spacecraft can be made early in the development, even for new boosters (Ref. 4). Early static firing data should also be available to check these estimates. Prediction of aerodynamic noise at transonic flight, however, is currently a more uncertain matter. Wind-tunnel model test data is problematic in nature, and analytic prediction techniques are not reliable.

A. Check of Prediction Against Actual Ranger Flight Data

To check the accuracy of this method of vibration prediction, the AA measured at the *Ranger* flight accelerometers in the spacecraft adapter are combined with an estimate of the liftoff acoustic environment; the results are then compared with actual measured liftoff vibration data. The liftoff acoustic field used for this prediction is the estimated PSL from Fig. 9. By combining this curve with the liftoff AA from Figs. 13 and 14, the vibration PSD's on Figs. 15, 16, and 17 were obtained. These are predictions for three types of flight accelerometers: the mounts from *Rangers I–IV*, *Rangers VI* and *VIII*, and *Ranger VII*. The actual liftoff flight data used for comparison has been replotted from Figs. 1, 3, and 5. The data from *Rangers I* through *IV* is an average of the four flights. The three figures show that the estimating technique predicts vibration levels very close in magnitude to those actually measured; there are, however, some discrepancies in frequency content. The *Ranger I–IV* prediction (Fig. 15) shows more vibration energy in lower frequencies than actually measured; this is also true for

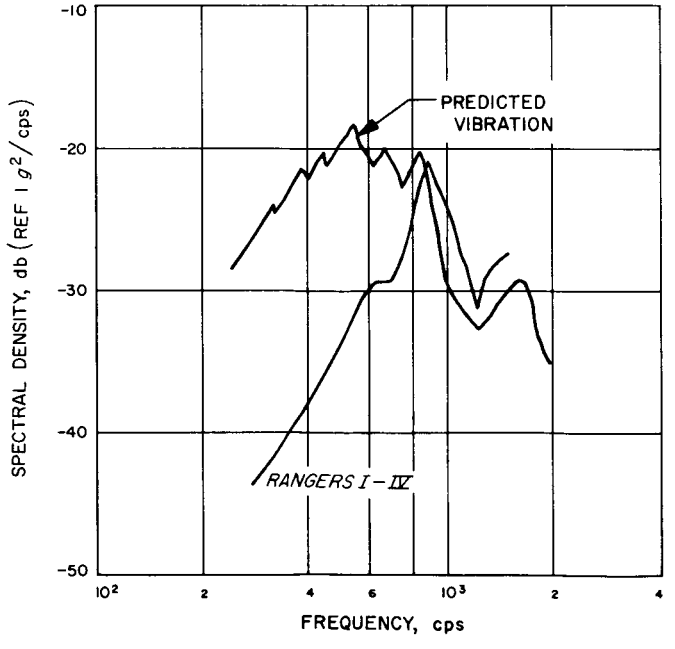

Fig. 15. Predicted and measured liftoff vibration: *Rangers I–IV*

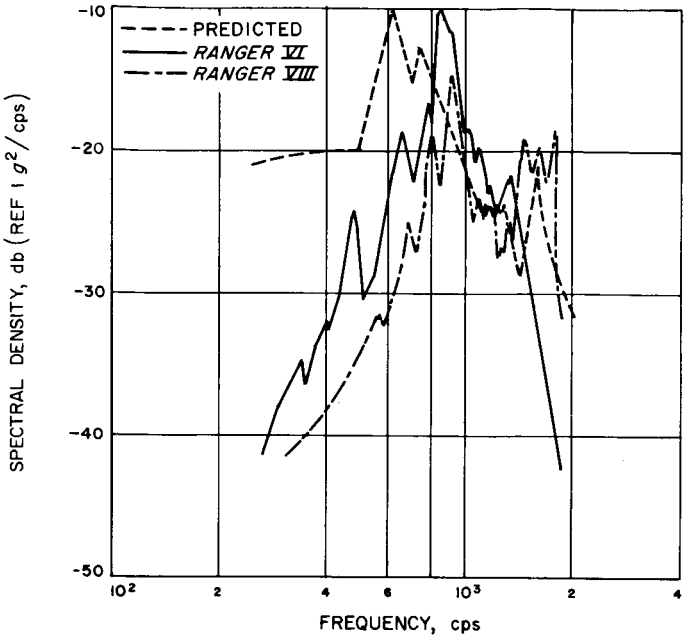

Fig. 16. Predicted and measured liftoff vibration: *Rangers VI and VIII*

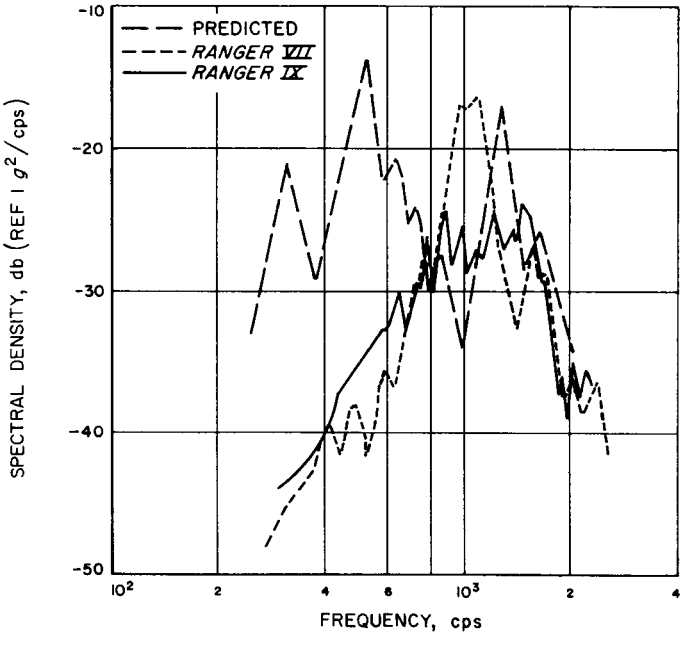

Fig. 17. Predicted and measured liftoff vibration: *Rangers VII and IX*

the *Ranger VII* estimate. In both cases, however, the peak value of the flight measurement would have been included by a broad frequency use of the predictions. (The estimate of vibration would have been conservative at low frequencies.) The *Ranger VI* estimate is better, but again would have been conservative.

The general conclusion resulting from this comparison of predicted levels to measured flight levels is that this method results in a reasonable prediction of the magnitude and general frequency content of flight vibration; however, exact frequency content is not predictable.

B. Vibration at Spacecraft Bus Flight Accelerometer Location

The measured vibration of an accelerometer in the spacecraft bus region from the *Ranger VIII* and *IX* flights is compared with a prediction of a general spacecraft bus vibration environment in Ref. 3. The prediction for the adapter accelerometers discussed previously is based on AA measurements in the spacecraft bus region and the Ref. 2 estimate of the liftoff acoustic environment. Fig. 15 shows the predicted and actual data from Ref. 3. The predicted band of vibration levels is the envelope of an average of 27 measurement points in the spacecraft bus. The flight data is from the *Ranger VIII* flight. The agreement of prediction with flight is similar to that found for the adapter accelerometers; the prediction is good at higher frequencies, but overly conservative at lower frequencies.

C. Inferences of an Equivalent Transonic Acoustic Field

The AA of Figs. 10, 11, and 12 indicate that the AA measured at the flight accelerometer is similar for both liftoff and transonic excitation; therefore, an "equivalent" transonic acoustic field may be calculated by multiplying the liftoff acoustic field by the ratio of measured transonic vibration to measured liftoff vibration. The equivalent transonic acoustic field PSL is shown in Fig. 18 along with the liftoff acoustic field PSL. The ratio of transonic to liftoff vibration used is the average of the ratios for the flights of *Rangers I* through *IV* and *Ranger VI*.

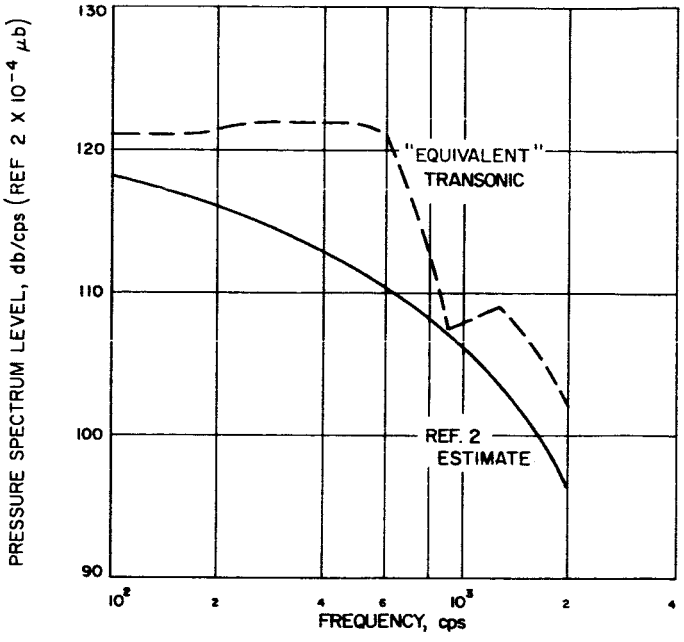

Fig. 18. Equivalent transonic acoustic field

It is important to note that this equivalent field is not a true measure of the transonic aerodynamic phenomenon (which, in reality, is a localized buffet or turbulent flow and, therefore, not really acoustic) but is, however, a measure of the acoustic field which, if applied to the spacecraft in the manner used in the ground test, would produce vibration at the flight accelerometers equal to that found during actual transonic flight conditions.

V. ESTIMATION OF FLIGHT VIBRATION LEVELS AT SPACECRAFT FEET

While flight vibration was measured on the flight adapter, the spacecraft vibration test was controlled as an input directly to the six spacecraft feet. To compare the spacecraft flight acceptance (FA) vibration tests with the actual flight environment, it is therefore necessary to estimate the in-flight spacecraft foot environment. It must be realized that the FA tests are intended to produce vibration damage potential greater than that expected to

occur on 95 out of 100 prospective spacecraft launches rather than to simulate the exact environments. A comparison of the flight and test environments will be made using a statistical estimate of the 95th percentile flight environmental PSD at the spacecraft feet and the specified vibration test PSD.

A. Method of Estimating: Spacecraft Foot Flight Vibration

The estimation technique is based on the use of data from the ground acoustic test. During the test, vibration levels were measured at the spacecraft feet as well as at the flight accelerometer locations. It has been shown (Ref. 3) that the ratio of vibration in the spacecraft bus region to the adapter region, as measured by the ground test, agrees well with the ratio of the bus accelerometer to adapter accelerometer on the *Ranger VIII* and *IX* vehicles. Therefore, it may be assumed that the distribution of vibration over the spacecraft and adapter during the ground test will be similar to that in flight. The ratio of vibration at the spacecraft feet to vibration at the flight accelerometer, as measured during ground test, may be used to convert measured flight vibration at the adapter to estimated flight vibration at the spacecraft feet.

The spectra ratios of Figs. 19 and 20 were used to compare estimated flight levels with the FA vibration tests. Since the liftoff and transonic simulations produce a similar ratio, only that determined by the transonic simulation was used. An overall evaluation of each ground test

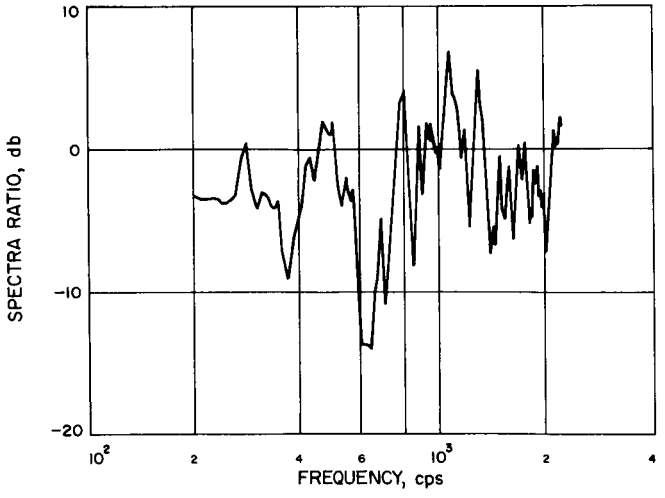

Fig. 19. Spectra ratio of vibration at spacecraft feet axial to *Ranger I–IV* flight accelerometer: transonic simulation

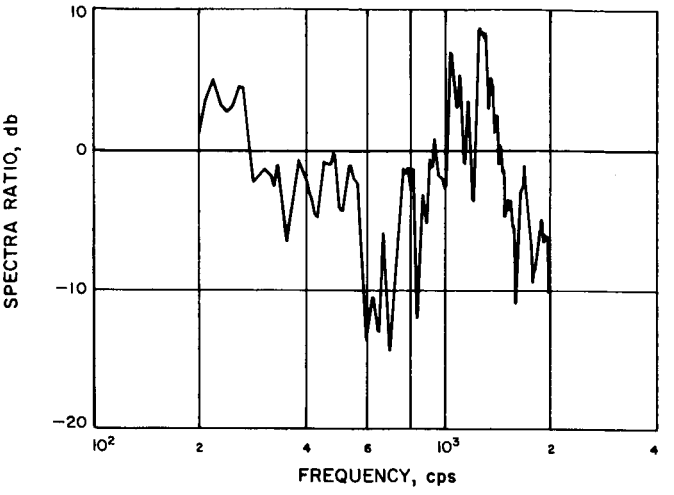

Fig. 20. Spectra ratio of vibration at spacecraft feet lateral to *Ranger I–IV* flight accelerometer: transonic simulation

simulation indicates that the transonic test is superior for this use. Figure 19 shows the ratio of the average spacecraft foot PSD (averaged in 20-cps wide frequency bands) in the axial direction to the PSD at the *Ranger I–IV* flight accelerometer location. The ratio is also determined

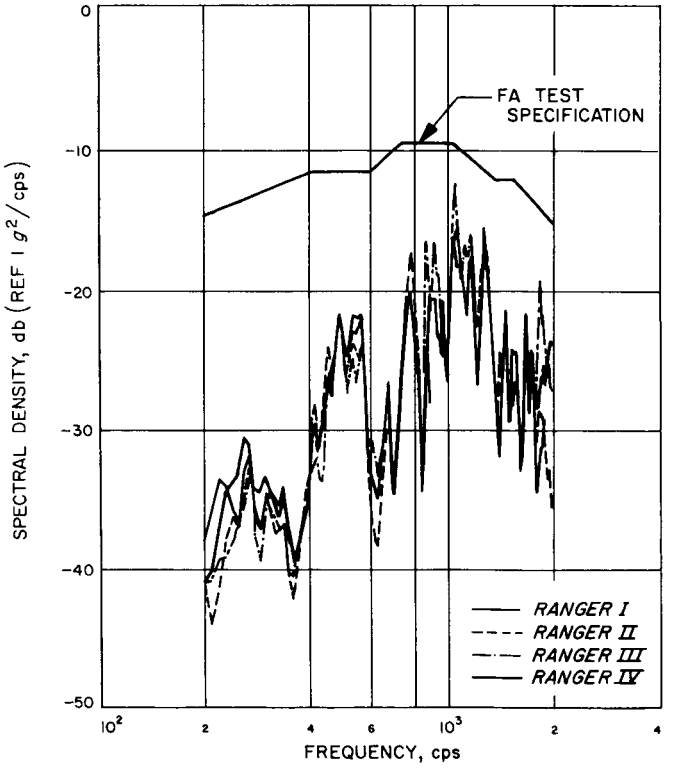

Fig. 21. Calculated *Ranger I–IV* vibration at spacecraft feet: axial

in 20-cps bandwidths. Figure 20 is a similar ratio, with the spacecraft foot the average of 12 lateral PSD's (six radial and six tangential). The power averages are used for comparison, since the FA vibration test specification and simulation techniques require control to the average power input to the spacecraft.

B. Estimated Flight Vibration at Spacecraft Feet

Spacecraft vibration tests are ultimately judged by the average PSD at the six spacecraft feet. The *Ranger I–IV* transonic data at the flight accelerometer (Fig. 2) may be transformed to estimated vibration at the spacecraft feet by using the ratios of Figs. 19 and 20. Only the transonic flight data is used because the liftoff data is lower except for a small peak at 900 cps. The resulting plots are shown in Figs. 21 and 22 along with the appropriate vibration specification. The test requirement adequately covers all flight data. In order to compare this data with the vibration specifications (since it is based on a 95th percentile flight), the four pieces of data have also been statistically analyzed (in 20-cps bands). The mean, 75th percentile, and 95th percentile log normal plots are compared with the specified PSD's in Figs. 23 and 24, which show the

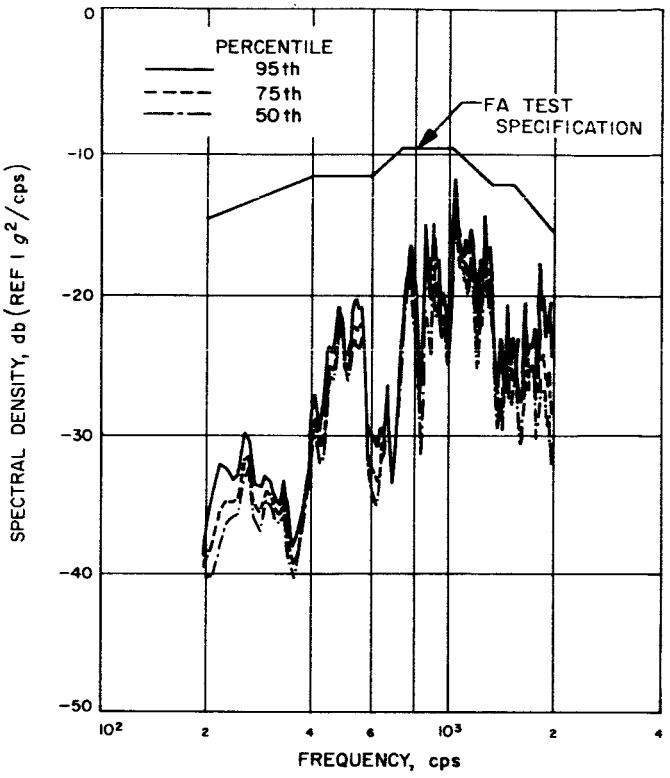

Fig. 23. Statistical analysis of *Ranger I–IV* vibration at spacecraft feet: axial

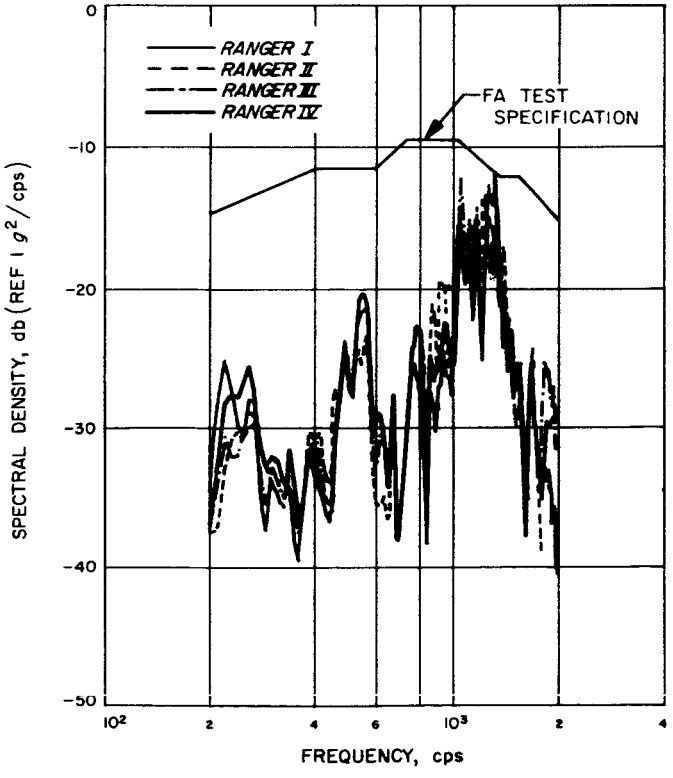

Fig. 22. Calculated *Ranger I–IV* vibration at spacecraft feet: lateral

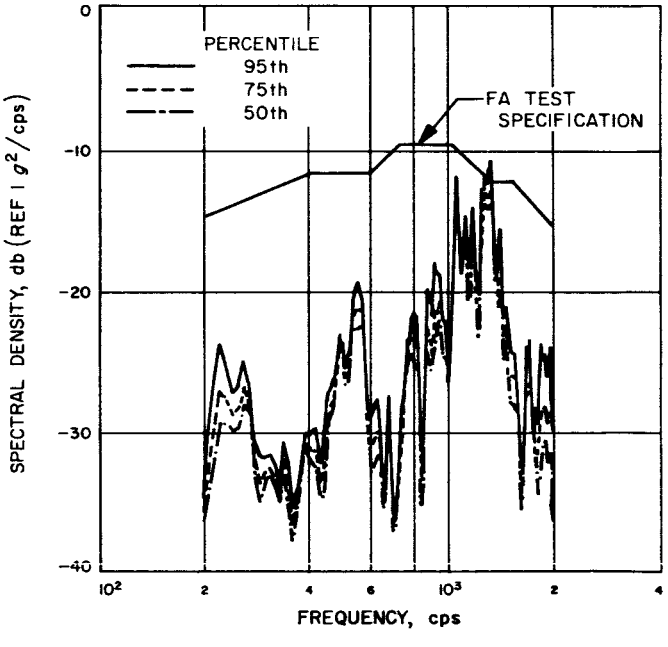

Fig. 24. Statistical analysis of *Ranger I–IV* vibration at spacecraft feet: lateral

FA test levels to be a reasonable approximation of the 95th percentile flight. In the axial direction (Fig. 23), the minimum margin of test over flight is 2 db at 1100 cps; at all other frequencies, the margin is greater. In the lateral direction (Fig. 24), the flight environment slightly exceeds the test at 1300 cps, but a margin exists at all other frequencies.

This same approach could be used with the *Ranger VI* and *VIII*, *VII* and *IX* data; however, the highly resonant characteristics of the mounting used on the *Ranger VI–VIII* flights and the lack of ground test data on the *Ranger IX* block make it impossible to accurately transform the spacecraft flight location data to spacecraft foot data. An attempt to use the *Ranger VI–IX* data is shown in Ref. 1. The results of the attempt to use the *Ranger VI–IX* transonic data are shown in Fig. 25. The effect of the higher frequency resonances in the mounting block is evident in the great variation between the *Ranger I–IV* data (Fig. 2) and *Ranger VI–IX* data (Fig. 25). Ideally, the ground test should be able to compensate for the mounting block resonances by using them as part of the transfer function computation (flight accelerometer to spacecraft feet). There are two reasons why this method does not work in practice:

(1) For sharp resonances, significant variance in measured gain can be expected when different mounting blocks are used or even if a test is repeated on the same block.

(2) When the mounting block is changed, small variances in the frequency of resonances greater than the 20-cps resolution of the PSD result in the ground test calculated gains being completely inaccurate for correction.

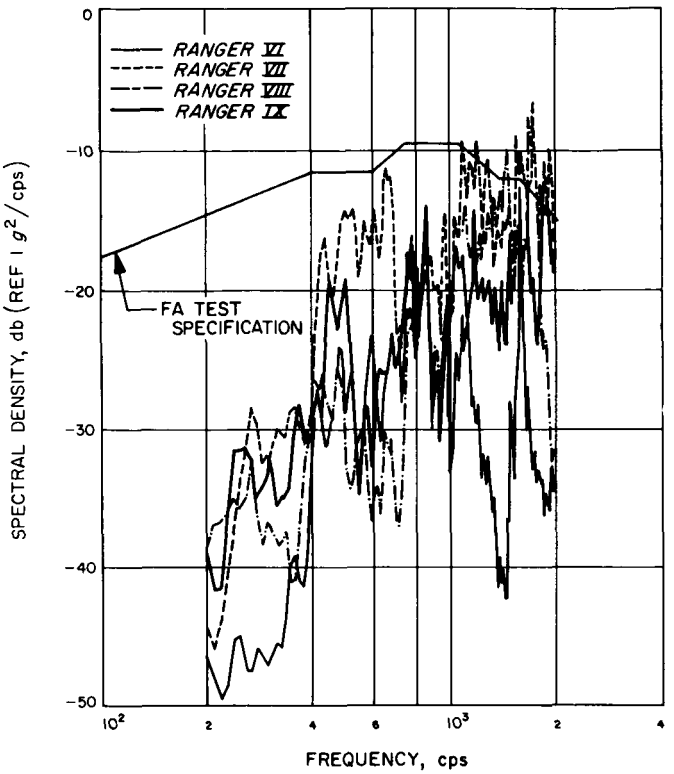

Fig. 25. Calculated *Ranger VI–IX* vibration at spacecraft feet: axial

For these two reasons, only the data from *Rangers I* through *IV* may be used for comparison of flight to test.

VI. ESTIMATION OF VIBRATION AT SPACECRAFT BUS ASSEMBLIES AND TV SUBSYSTEM

The technique is similar to that applied to the spacecraft foot estimate. By using a similar vibration excitation mechanism, the ground acoustic test may be used to compare vibration in the various locations of the spacecraft; flight data at one location may then be converted to an estimate of in-flight vibration at another location. To represent a distribution over the spacecraft and TV subsystem, 40 accelerometer locations on the six spacecraft bus assemblies and 18 accelerometer locations on the TV subsystem were considered.

A. Gains to Spacecraft Bus and TV Subsystem

Figures 26 and 27 show the ratios of the average PSD's on the spacecraft bus assemblies and TV subsystem to the average PSD on the spacecraft feet (lateral direction). The averages and ratios are determined in 20-cps wide frequency bands. The estimates of the 95th percentile flight vibration at the spacecraft bus and TV subsystem were obtained by using the 95th percentile foot estimate from *Rangers I* through *IV* (Fig. 25) and the spectra ratios from Figs. 26 and 27. The spacecraft flight estimates are shown in Figs. 28 and 29. The assembly level FA vibration test is more than 24 db above the flight estimate for both the spacecraft bus assemblies and TV subsystem. While the margin of test over flight environment is high, the assembly environment experienced during system level vibration test has not been discussed. In actuality, the assembly level vibration test was intended to include

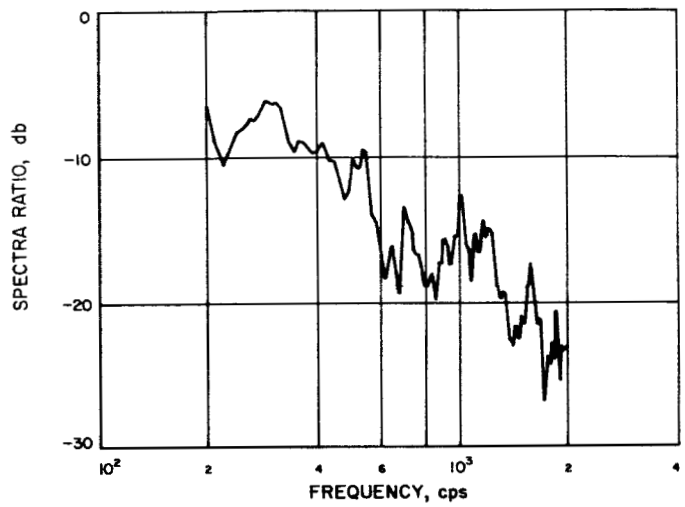

Fig. 26. Spectra ratio of average vibration of spacecraft bus assemblies to the average spacecraft foot vibration: lateral

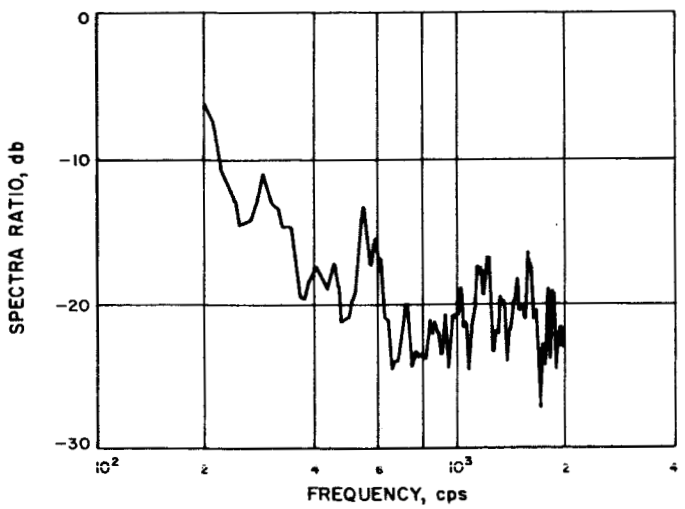

Fig. 27. Spectra ratio of average vibration of TV subsystem to the average spacecraft foot vibration: lateral

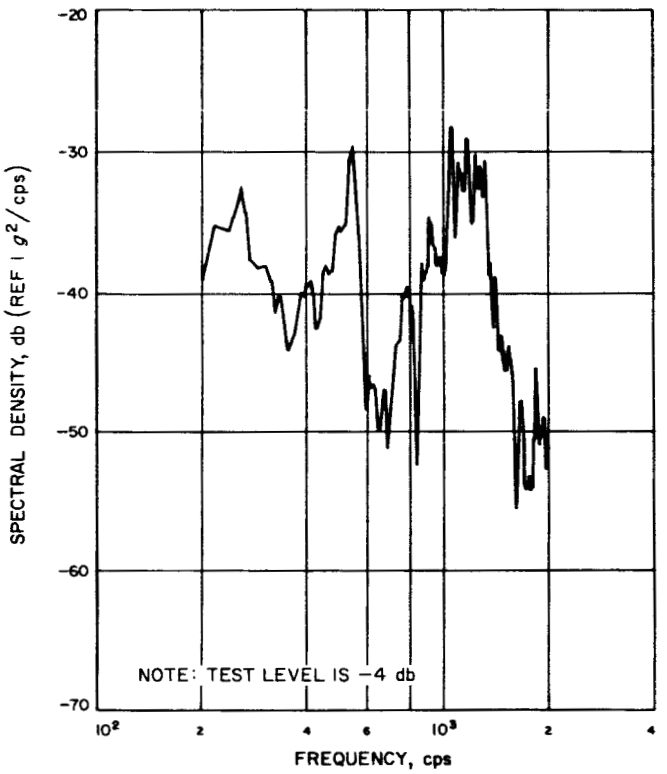

Fig. 28. Calculated 95th percentile flight vibration at spacecraft bus assemblies

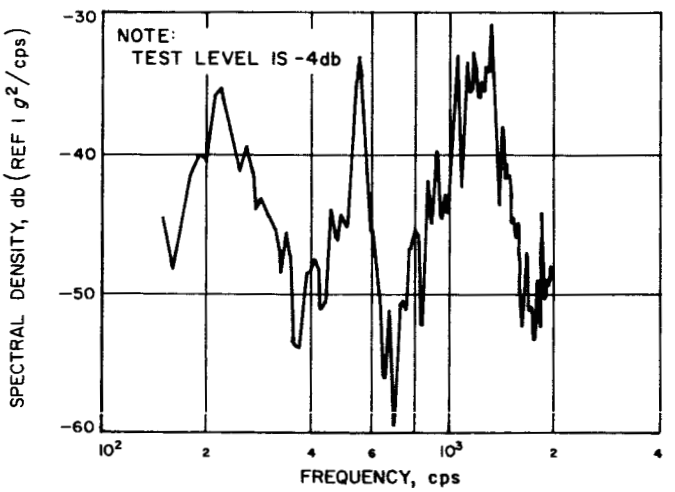

Fig. 29. Calculated 95th percentile flight vibration at TV subsystem

the spacecraft system test environment as well as the flight environment. The measured vibration gain from the spacecraft feet to the spacecraft bus assemblies and TV subsystem is greater in the vibration test configuration than in the in-flight configuration. Therefore, for a given vibration level at the spacecraft feet, the bus assemblies and TV subsystem levels will be higher in test than in flight. The difference in gain is due to such factors as greater source mechanical impedance in the vibration test configuration; cross-axis input during vibration test; and vibration test-fixture resonances.

In Ref. 3, Fig. 8, another ratio of vibration in two regions of the spacecraft, obtained from the ground test data, is shown to compare favorably with a similar ratio measured during flight. The comparison is between the ratios of the spacecraft bus flight accelerometer to the adapter flight accelerometer (as determined from *Ranger VII* flight data) and the average spacecraft bus assembly PSD to the average adapter PSD (as determined from the ground test). The similarity of these ratios indicates that this method of estimating assembly level vibration is reasonable.

VII. CONCLUSIONS

Some restrictions imposed by the small amount of available flight vibration data from the *Ranger* Project were overcome by the use of a ground acoustic simulation of the vibration excitation mechanisms at liftoff and transonic flight. The data from the ground test was used in conjunction with the flight data to produce the following results:

(1) By comparing vibration in various parts of the spacecraft, the two modes of vibration excitation were found to have no apparent effect on the distribution of vibration over the spacecraft. The changes in flight accelerometer mounting blocks were shown to have a great effect on the measured vibration response to an identical exciting field, apparently due to mounting block resonances on the *Ranger VI–VIII* blocks.

(2) Acoustic acceptances for use in estimating expected vibration on other spacecraft were calculated from ground test data. Vibration level predictions using this technique were compared with actual *Ranger* flight data and found to be reasonable at higher frequencies; they are, however, overly conservative at lower frequencies.

(3) The flight vibration data was used with the ground test data to estimate flight vibration levels at the spacecraft feet. The flight data from *Rangers VI–VIII* was found to be unusable for this purpose because of resonances in the accelerometer mounting blocks. Results from the *Ranger I–IV* flights were statistically analyzed; the spacecraft vibration test levels were shown to be reasonably consistent with the 95th percentile spacecraft flight vibration levels.

(4) Estimates were made of in-flight vibration levels on spacecraft bus assemblies and on the TV subsystem. Using a 95th percentile flight vibration level and an average assembly location, there was an indicated margin of 24 db of assembly level vibration over flight environment.

REFERENCES

1. Wiksten, D. B., *Dynamic Environment of the Ranger Spacecraft: I through IX (Final Report)*, Technical Report No. 32-909, Jet Propulsion Laboratory, Pasadena, Calif., May 1, 1966.

2. *Noise and Noise-Induced Structural Vibration of the Ranger Spacecraft*, Report No. 1038A, Bolt, Beranek and Newman, Inc., May 20, 1965.

3. Trummel, M. C., *Ground Test Simulation of Lift-off and Transonic Vibration Excitation Mechanisms on the Ranger Spacecraft*, Technical Memorandum No. 33-256, Jet Propulsion Laboratory, Pasadena, Calif., November 1, 1965.

4. Crandall, S. (editor), *Random Vibration*, John Wiley & Sons, New York, 1958.